# Diffusion and nuclear magnetic relaxation of $H_2$ in rare-gas liquids

Mark S. Conradi,* K. Luszczynski, and R. E. Norberg
*Department of Physics, Washington University, St. Louis, Missouri 63130*
(Received 17 July 1978)

Pulsed NMR has been used to study $H_2$ as a dilute impurity in the rare-gas liquids neon, argon, and krypton. $H_2$ diffusion was measured and is compared to the somewhat smaller self-diffusion of the hosts. The temperature dependences of the impurity and host diffusions are the same (and nearly Arrhenius) in the cold liquids. At temperatures approaching the critical temperature, the impurity diffusion is a more rapidly increasing function of temperature than is the host diffusion. The $H_2$ impurity diffusion is compared with predictions of molecular dynamics. Proton relaxation times $T_1$ and $T_2$ also were measured and are compared with proton relaxation measurements in gaseous dilute $H_2$–rare-gas mixtures, and in dilute ortho-$H_2$–para-$H_2$ fluid mixtures. The relaxation results are compared with some predictions of the theory of Bloom and Oppenheim.

## I. INTRODUCTION

Diffusion and spin relaxation in the rare-gas liquids and in liquid hydrogen have been the subjects of many reported experimental and theoretical studies. However, there are few reported results on the diffusion and relaxation of dilute impurities in rare-gas liquid hosts. In the present work dilute molecular hydrogen ($H_2$) has been studied in liquid krypton, argon, and neon. Pulsed proton magnetic resonance was used to measure the nuclear-spin relaxation times and the diffusion coefficients of the orthohydrogen ($o$-$H_2$) component of the impurities. The measurements extend over nearly the entire liquid-temperature intervals, near the saturated-vapor-pressure (SVP) curves of the host liquids. The $H_2$ concentrations used were less than 1% with an ortho-para ratio of 3:1. The experimental results are found to be essentially independent of the $H_2$ concentration, and reflect the behavior of isolated $o$-$H_2$ molecules in liquid-rare-gas hosts.

The diffusion data reported here are believed to be unique among the reported impurity diffusion data in simple liquids, principally because of the wide temperature range examined. Pronounced deviations of the $H_2$ diffusion from the usual Arrhenius thermally activated temperature dependence are observed at the higher temperatures. The present study of one impurity in a sequence of rare-gas host liquids complements previous diffusion studies of different impurities in a single host.[1-3]

The nuclear magnetic relaxation of dilute $H_2$ in the liquid solutions arises from the intramolecular dipolar spin-spin coupling and the intramolecular spin-rotation coupling, both modulated by the rotational motion of the $H_2$ molecule. Consequently, the relaxation data reported here are measures of the correlation times of the $H_2$ molecular angular momenta. The relaxation data from the liquids are compared with gas-phase results reported for dilute $H_2$–rare-gas mixtures[4,5] and with results from gas and liquid dilute mixtures of $o$-$H_2$ in $p$-$H_2$.[6,7]

A subsequent paper[8] will report experimental results obtained for dilute $o$-$H_2$ in solid neon, argon, krypton, and $p$-$H_2$.

## II. EXPERIMENTAL DETAILS

Dilute solutions of $H_2$ in rare-gas liquids were produced using the vapor-recirculation technique previously used in gas-liquid, two-component equilibrium studies.[9,10] In this method, the gas phase of the system is recirculated (bubbled) through the liquid phase until equilibrium is reached. The recirculation pump used was a modification of Sterner's design.[11] Also, a thermal flow gauge was constructed, based upon previous design.[12] The sample chamber had two sections joined by a thin vertical neck. This unusual design was chosen so that the liquid-vapor meniscus could be adjusted to lie in the upper (copper) section. The copper shielded this section from the rf field of the NMR coil, which was wound around the lower chamber (made of proton-free Kel-F plastic). Thus no NMR signals from the gas phase of the system were present.

Solutions were produced in the following manner. Pure-rare-gas solvent was condensed in the sample chamber, filling all of the lower section and about half of the upper section. Then $H_2$ gas was admitted into the gas phase of the system and the recirculation pump was started. After about 2 min, observation of the $H_2$ NMR signal indicated that an equilibrium concentration of $H_2$ had been obtained. Typically, the pump was run for about 10 min, to

 

ensure equilibrium. The pump was always off during data accumulation and for at least 10 min prior to data taking. This allowed bubbles to escape from the lower section and also removed macroscopic flow.

The sample gases for these experiments were purchased in small cylinders at high pressures, to allow the gases to be moved under their own pressure. Hydrogen and argon were obtained from Air Products Corp. The argon was "ultrahigh purity" (impurities stated to be in the low-ppm level) and the $H_2$ was "chemical purity" (about ten times more impurities). All the other experiments used Linde "research-grade" gases (low-ppm impurity levels).

$H_2$ concentrations were measured by two methods. In the first method, the initial amplitude of the free-induction decay was measured for a particular solution. Having previously (at the start of each run) calibrated the NMR sensitivity with a $H_2$-gas sample of known pressure, the $H_2$ concentration in solution was calculated. This calculation assumed a Curie temperature dependence of magnetization and ideal-gas behavior for the $H_2$-gas calibration sample. The second method was to use the gas-liquid equilibrium data available for $H_2$ in neon[9] and for $H_2$ in argon.[10,13] Knowledge of the temperature and total pressure at equilibrium is sufficient to determine $H_2$ concentrations in both the gas and the liquid according to Gibbs' phase rule. These two methods agreed to within 20%, which is satisfactory in view of the near absence of any concentration dependences in the data. All concentration values reported here are obtained from the NMR method. The concentrations stated refer to total $H_2$ (ortho and para) content. The NMR method measures only $o$-$H_2$, and the room-temperature ortho-para ratio of 3:1 has been assumed throughout. No evidence was seen for ortho-para conversion in these solutions, and none was expected in such dilute nonmagnetic systems.

The phase-coherent pulsed NMR apparatus operated at 20 MHz and employed a single rf coil. The transmitter followed the design of Clark,[14] with gating pulses produced by a digital, crystal-controlled timing unit. The receiver utilized phase-coherent detection, in order to optimize the detection of signals buried in noise.[15,16] A room-temperature field-effect-transistor preamplifier was employed. The magnetic field was stabilized with a $^{19}F$ field-locking continuous-wave NMR apparatus. Because the dilute samples produced weak proton NMR signals, extensive use was made of signal averaging. Generally, from 100 to 1500 waveforms were averaged for each measurement of echo or induction decay amplitude.

The magnetic field gradient for the diffusion measurements was supplied by an (approximately) anti-Helmholtz coil pair in the gap of the iron-yoke electromagnet.[17] The ratio of gradient to current for the coils was measured with a water sample in a separate experiment. The gradient value was determined from the time width of spin echoes from the water, following Murday's analysis.[18] This calibration, estimated to be accurate to ±2%, leads to a ±4% uncertainty in the individually measured diffusion coefficients.

The spin-lattice relaxation times $T_1$ were measured using a $180°$-$\tau$-$90°$ inversion-recovery sequence. The transverse relaxation times $T_2$ and diffusion coefficients $D$ were measured with a $90°$-$\tau$-$180°$ echo generating sequence. In all cases, the $\tau$ dependence of the amplitude of the resulting induction decays or echoes fit well to the appropriate Bloch relaxation expressions. The scatter in the measured values of $T_1$, $T_2$, and $D$ depended on the $H_2$ concentration, because of signal-to-noise reasons. However, $T_1$ and $T_2$ typically were measured to ±3%, while $D$ was measured to ±6%. The extra uncertainty in $D$ measurements arises from the wider receiver bandwidth necessary to observe the spin echoes with a dc field gradient applied.

The low-temperature probe contained a vapor-flow cooling scheme, which used the boil-off gas from the research Dewar and proved economical and easy to adjust. Temperature regulation was provided by a commercial regulator, in connection with a heater wound around the heat exchanger of the vapor-flow circuit. Temperature measurement was performed by a dc potentiometric scheme with a carbon-in-glass resistance thermometer. This thermometer proved stable to within our ability to detect calibration changes (about 0.15 K at 100 K). The resistor was calibrated against the vapor pressures of liquid helium, hydrogen, neon, argon, and krypton. The calibration showed good consistency where overlap of the calibrating liquids occurred. The temperatures quoted here are believed accurate to ±0.15% for argon and krypton, and ±0.15 K for neon.

## III. DIFFUSION

The experimental results for diffusion of dilute $H_2$ in liquid krypton, argon, and neon are shown in Figs. 1–3. The data are plotted with a reduced abscissa $1/T^* = T_t/T$. Here $T_t$ is the triple-point temperature of the pure host (24.55, 83.81, and 115.76 K for neon, argon, and krypton, respectively[19]). The results do not appear to depend on $H_2$ concentration, and may be taken to represent the diffusion of isolated $H_2$ molecules in otherwise pure rare-gas liquids.

Figures 1–3 also include, for comparison, reported self-diffusion results in the host liquids. These include the SVP-neon NMR results of Henry and Norberg[20] and 10-atm-neon tracer data of Bewilogua, Gladun, and Kubsch,[21] some 12.9-atm-argon and 8.48-atm-krypton tracer results of Naghizadeh and Rice,[22] and the SVP-krypton NMR data of Cowgill and Norberg.[23] Figure 2 also shows tracer results for the diffusion of HT in argon.[1] The critical temperatures are indicated at the left-hand side of the figures.

The only previously reported measurements of $H_2$-impurity diffusion in rare-gas liquids also are indicated. These are single points obtained[24] from neutron scattering in liquid argon at 100 K, 27 atm, and 3.3% $H_2$ and in liquid neon at 26 K, 2 atm, and 1.5% $H_2$. The two values disagree with the data reported here by amounts larger than the stated errors. The disagreements are in opposite directions for neon and argon. The discussion that follows will refer to the present NMR results for $H_2$-impurity diffusion.

The behavior of the $H_2$ diffusion in the three liquids is similar. At low temperatures, such that $1/T^*>0.75$, the $H_2$ diffusion parallels the temperature dependence of the self-diffusion in Figs. 1–3. In the cold liquids both the $H_2$ diffusion and the self-diffusion approximately obey Arrhenius relations with the same activation energy for the $H_2$ diffusion and the self-diffusion in each case. However, the $H_2$ diffusion coefficient is systematically larger than the host self-diffusion coefficient. At higher temperatures both the $H_2$ diffusion and the self-diffusion (where data exist) deviate upwards from an Arrhenius behavior, with the $H_2$ diffusion increasing more rapidly with increasing temperature than does the self-diffusion. Other workers previously have noted[1,3] the parallel low-temperature behavior of impurity and host diffusion in liquids near the triple point. However, the rapid increase in light-impurity diffusion in simple liquids at high temperatures does not appear to have been reported previously. Qualitatively, the increase in the ratio of impurity to self-diffusion at high temperatures is to be expected. At sufficiently low densities the liquid mixture should be similar to a gas mixture, where the diffusion ratio would be large because of the light mass of the hydrogen.

The $H_2$ diffusion and host self-diffusion for liquid krypton may be compared in detail, since in this case the NMR measurements of self-diffusion at

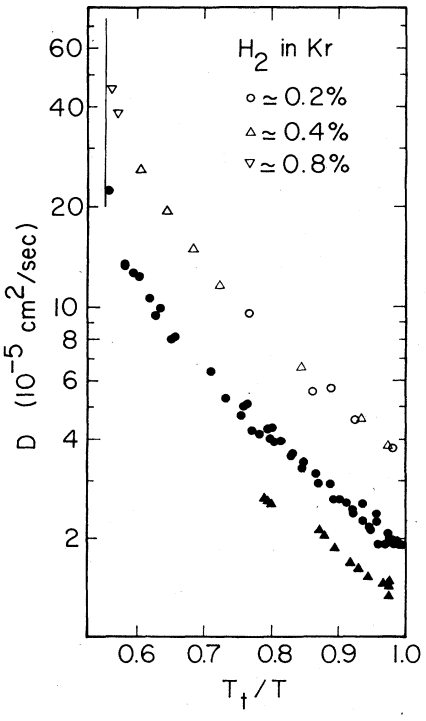


FIG. 1. Diffusion of dilute $H_2$ in liquid krypton (open symbols). ● , krypton self-diffusion (NMR, Ref. 23). ▲, krypton self-diffusion (tracer, Ref. 22).

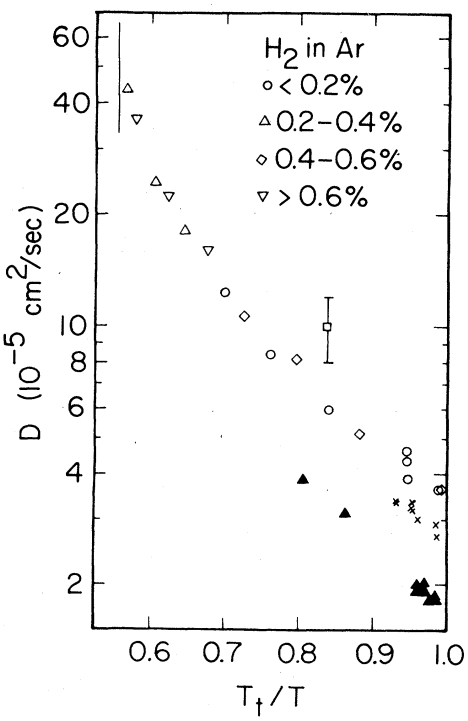


FIG. 2. Diffusion of dilute $H_2$ in liquid argon (open symbols). ▲, argon self-diffusion (tracer, Ref. 22). ×, diffusion of HT in argon (tracer, Ref. 1). □, $H_2$ in argon (neutron scattering, Ref. 24).

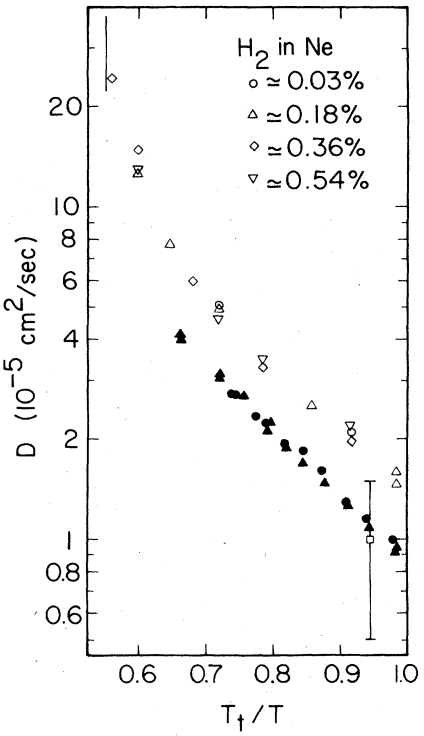


FIG. 3. Diffusion of dilute $H_2$ in liquid neon (open symbols). ●, neon self-diffusion (NMR, Ref. 20). ▲, neon self-diffusion (tracer, Ref. 21). □, $H_2$ in neon (neutron scattering, Ref. 24).

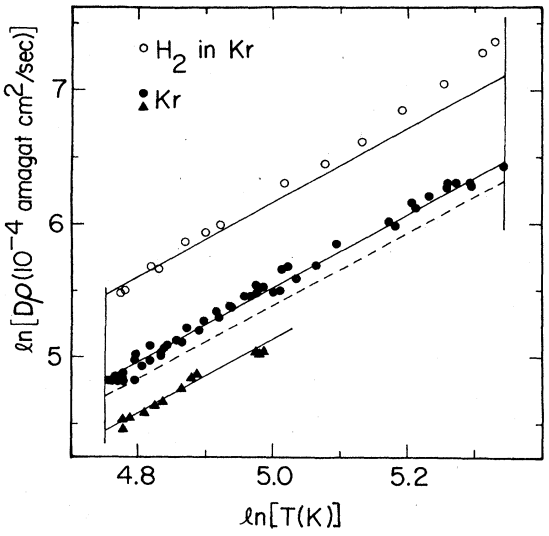


FIG. 4. Temperature variation of $D\rho$ for liquid krypton. ○, $H_2$ diffusion in krypton. ●, ▲, krypton self-diffusion (Refs. 22 and 23). The dashed line indicates the classical corresponding states self-diffusion prediction based on xenon results of Ref. 26.

SVP extend to the critical point. Nevertheless, comparison of the results shown in Fig. 1 is made difficult by the deviation from activated temperature dependence and by the rapid variation of both diffusion coefficients in the vicinity of the critical point. The temperature range of the argon self-diffusion data is very limited, and these results, like the neon tracer data, were obtained at constant pressure rather than at SVP, while the present $H_2$ impurity diffusion measurements are taken near SVP.

However, what appear to be reliable NMR measurements of self-diffusion have been reported for liquid xenon at SVP to the critical point.[25,26] Ehrlich and Carr[26] have observed that their liquid-xenon diffusion results can be fitted well over nearly the entire liquid-gas coexistence curve by the empirical power-law relation

$$D\rho = aT^{2.74\pm0.08}, \quad (1)$$

where $\rho$ is the liquid density and $a$ is a constant. A similar expression has been employed to fit diffusion results in liquid ethane[27] and methane.[26] If Eq. (1) can be shown to describe the available self-diffusion data in liquid neon, argon, and krypton, then comparison with the $H_2$ impurity diffusion becomes simpler.

Figures 4–6 show the data of Figs. 1–3 replotted as $\ln 10^4 D\rho$ vs $\ln T$, with $\rho$ in amagats for the pure liquids.[19,28] The amagat is a unit of relative density. 1 amagat corresponds to the gas at 0 °C and 1 atm, and for the rare gases used here is Kr, 3.7493 g liter$^{-1}$; Ar, 1.784 03 g liter$^{-1}$; Ne, 0.899 94 g liter$^{-1}$.[28] The triple and critical temperatures are indicated, and the sloping straight lines all have been drawn with a slope of 2.74. It is evident that Eq. (1) gives a reasonably good description of the self-diffusion results in liquid krypton, argon, and neon. In addition, Figs. 4–6 show that there is a systematic deviation between the $H_2$-impurity diffusion and the host self-diffusion in the hot liquids.

Figure 4 shows that $T^{2.74}$ fits the krypton self-diffusion $D\rho$ results well over the entire liquid range. The solid lines are drawn through the NMR and tracer data which disagree by a constant factor. The dashed line indicates the results of the application of the classical theory of corresponding states to a calculation of $D$ for krypton, based on the Ehrlich and Carr results[25,26] for diffusion in liquid xenon, which also agree well with the earlier tracer results[22] for xenon. The upper solid line has been fitted, as a guide to the eye, to the $H_2$ in krypton $D\rho$ data at low temperatures. A least-squares fit of Eq. (1) to the krypton NMR self-diffusion $D\rho$ data (solid dots) in Fig. 4 yields an exponent of $2.87 \pm 0.04$. Nevertheless, the lines

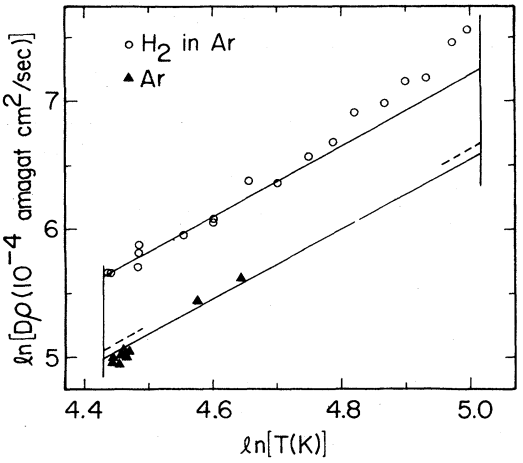


FIG. 5. Temperature variation of $D\rho$ for liquid argon. O, $H_2$ diffusion in argon. ▲, argon self-diffusion (Ref. 22). The dashed end points indicate the classical corresponding states self-diffusion predicted based on xenon results of Ref. 26.

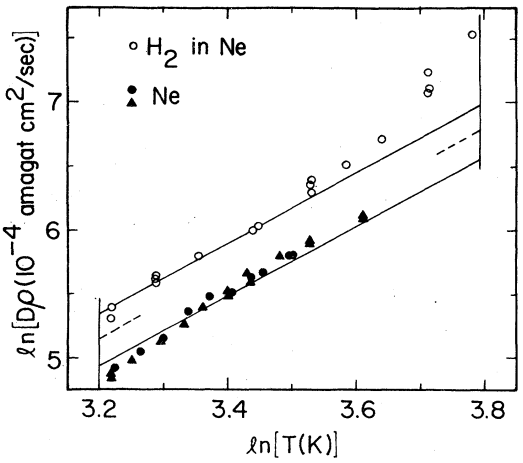


FIG. 6. Temperature variation of $D\rho$ for liquid neon. O, $H_2$ in neon. ●, ▲, neon self-diffusion (Refs. 20 and 21). The dashed end points indicate the classical corresponding states self-diffusion prediction based on xenon results of Ref. 26.

in Fig. 4 have been drawn with a slope corresponding to the reported[26] xenon result, 2.74.

The heavier rare gases form a set of physical systems to which the classical principle of corresponding states may be applied. Argon, krypton, and xenon should correspond almost classically,[29] while quantum effects in neon can produce appreciable deviations from classical correspondence.[20] The dashed lines in Figs. 4–6 have been determined from the xenon experimental self-diffusion results[25,26] by employing the scaling relation

$$D^* = \sigma(kT_t/m)^{1/2}[(m/kT_t)^{1/2}D/\sigma]_{Xe}\,, \qquad (2)$$

where $m$ is the atomic mass and $\sigma$ an atomic size taken to be one-half of the interatomic separation at the minimum of the interaction potential.[30] If the classical corresponding-states hypothesis is valid, then Eq. (2) is equivalent to the usual reduction of the diffusion coefficient[29]

$$D^* = (m/\epsilon)^{1/2}(1/\sigma)D\,, \qquad (3)$$

where $\epsilon$ is the pair-interaction well depth, which, however, depends on the model chosen for the pair potential.

The dashed end-point lines in Fig. 5 show the argon classical corresponding-states self-diffusion results based on the Ehrlich and Carr[25,26] xenon data. The corresponding-states result for argon is in reasonably good agreement with the solid line drawn through the argon self-diffusion data. A similar xenon-based classical corresponding-states line for neon lies (as indicated by the dashed end-point lines) significantly above the solid line drawn through the neon data in Fig. 6. The displacement may indicate the effect of quantum-mechanical terms needed for correspondence in liquid neon. The deviation from classical correspondence in liquid neon is much less than that reported for self-diffusion in solid neon.[20] It is apparent that an optimum power-law fit to the limited neon and argon self-diffusion $D\rho$ data might require a larger exponent than 2.74. However, in the absence of experimental data near the neon and argon critical points, the following analysis is based on employment of 2.74 as the exponent for the self-diffusion $D\rho$ behavior in liquid krypton, argon, and neon. With this assumption it becomes easy to compare the impurity diffusion and the self-diffusion over the entire liquid ranges.

Figure 7 presents such a comparison. The open symbols indicate values of the ratio $R$ obtained by dividing the hydrogen-impurity-diffusion data points of Figs. 4 and 6 by the corresponding values of the dashed line for krypton self-diffusion and the solid line for neon self-diffusion. The argon ratio points based on the solid line for argon self-diffusion in Fig. 5 lie between the neon and krypton ratios, and have been omitted for the sake of clarity. The curved lines in Fig. 7 indicate ratios obtained by drawing smooth curves through the hydrogen diffusion data of Figs. 4–6 and calculating ratios as before. For neon and argon the calculated diffusion ratios have been based on the $D\rho$ lines from the experimental self-diffusion data. For krypton the calculations have been based on the corresponding states self-diffusion $D\rho$ dashed line, because of

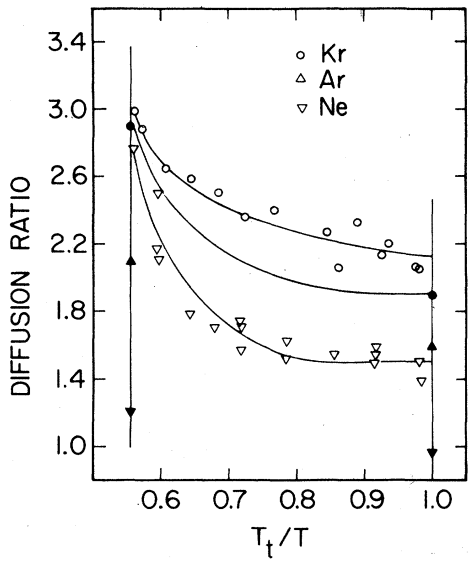


FIG. 7. Ratio of $H_2$ diffusion to self-diffusion in liquid neon, argon, and krypton. Solid symbols refer to molecular-dynamics calculations.

the disagreement between the two sets of krypton self-diffusion experimental data. It seems likely that the reported krypton NMR results[23] for self-diffusion are about 13% too large. Preliminary results from experiments currently in progress on $H_2$ in liquid xenon indicate diffusion ratios near the triple point to be somewhat larger than those shown for krypton in Fig. 7, in agreement with the trend established for the three systems reported here.

Alder, Alley, and Dymond[31] have performed molecular-dynamics computer experiments for a single impurity in an otherwise pure host fluid. All particles were assumed to interact with hard-sphere potentials. Results were reported as ratios of the computer-generated diffusion to the prediction of the Enskog theory. Table I presents some of the computer results converted to the ratio $R$ of impurity diffusion to host diffusion.[31] In Table I, $\sigma^\dagger$ represents the ratio of the diameters of the impurity atom and host atoms and $m^\dagger$ is the impurity mass divided by the host mass. The volume $V$ is divided by $V_0$, the close-packed volume of the spheres. The triple point in rare gases occurs at about $V/V_0 = 1.5$, and the critical point is near $V/V_0 = 3$.

The sizes of Ne, Ar, Kr, and $p$-$H_2$ are 2.79, 3.40, 3.62, and 2.96 Å, respectively.[19,32,33] Thus $H_2$ in neon, argon, and krypton corresponds to $\sigma^\dagger = 1.06$, 0.87, and 0.82. The mass ratios $m^\dagger$ are 0.10, 0.050, and 0.024. A smooth-curve interpolation between the ratios in Table I yields values

TABLE I. Hard-sphere molecular-dynamics results.

| | | Diffusion ratio $R$ | |
|---|---|---|---|
| | $m^{\dagger\,b}$ | $V/V_o = 3$ | $V/V_o = 1.6$ |
| $\sigma^{\dagger\,a} = 1$ | 1 | 1.00 | 1.00 |
| | 0.1 | 1.45 | 1.20 |
| | 0.01 | 2.08 | 1.28 |
| $\sigma^{\dagger\,a} = \frac{3}{4}$ | 1 | 1.35 | 1.57 |
| | 0.1 | 2.26 | 2.08 |
| | 0.01 | 4.37 | 2.01 |
| $\sigma^{\dagger\,a} = \frac{1}{2}$ | 1 | 1.97 | 2.89 |
| | 0.1 | 3.74 | 4.39 |
| | 0.01 | 9.04 | 7.64 |

[a] $\sigma^\dagger \equiv$ (impurity diameter)/(solvent diameter).
[b] $m^\dagger \equiv$ (impurity mass)/(solvent mass).

at these $\sigma^\dagger$ and $m^\dagger$ for $H_2$ in neon, argon, and krypton. The resulting values of $R$ near $T_t$ and $T_c$ are listed in Table II, along with the presently observed ratios at $T_t$ and $T_c$, from Figs. 4–6. The molecular-dynamics values from Table II also are indicated in Fig. 7 as solid symbols at the triple and critical temperatures.

The ratios of $H_2$ impurity diffusion to host diffusion reported here and the molecular-dynamics results are in better agreement near the triple points than near the critical points. This is a reasonable situation since at large densities the diffusion processes in fluids are controlled by the hard repulsive forces, and it has been shown[34,35] by molecular dynamics that the diffusion coefficient of the Lennard-Jones fluid is within 10% of that for the hard-sphere fluid. At lower densities the effect of the attractive potential should become more important and hard-sphere calculations less appropriate.

In both the present experiments and in the computer results, the diffusion ratios increase as $\sigma^\dagger$ (the impurity to host size ratio) decreases and also as temperature is increased from the triple point to the critical point. However, the observed

TABLE II. Comparison of calculated and observed values of diffusion ratio $R$.

| | Molecular dynamics | | Present Experiments | |
|---|---|---|---|---|
| | $R$ near $T_c$ | $R$ near $T_t$ | $R_c$ | $R_t$ |
| $H_2$-Ne | 1.2 | 0.96 | 2.9 | 1.5 |
| $H_2$-Ar | 2.1 | 1.6 | 3.0 | 1.9 |
| $H_2$-Kr | 2.9 | 1.9 | 3.1 | 2.1 |

ratios are systematically somewhat larger than the computer results. For krypton the observed and calculated ratios differ by less than 10% at both $T_t$ and $T_c$. Turning to argon and neon, one sees that the observed diffusion ratios at the critical point are nearly the same as for krypton, in contrast to the variation predicted by the computer results. For $H_2$ in neon the variation of the diffusion ratio with temperature is significantly larger than predicted from the classical hard-sphere molecular dynamics. Some of this apparent disagreement could arise from an incorrect choice of $D\rho \propto T^{2.74}$ for the neon self-diffusion. However, even a steeper power-law line fitted to the self-diffusion $D\rho$ data in Fig. 6 and corresponding to $T^{3.2}$ yields neon critical- and triple-point ratios of 2.4 and 1.6, and the ratio variation with temperature remains larger than calculated from molecular dynamics. More quantitative comparisons would require self-diffusion measurements to the critical point in liquid neon and argon and computer analyses performed for the actual values of $\sigma^\dagger$ and $m^\dagger$ and many values of relative volume.

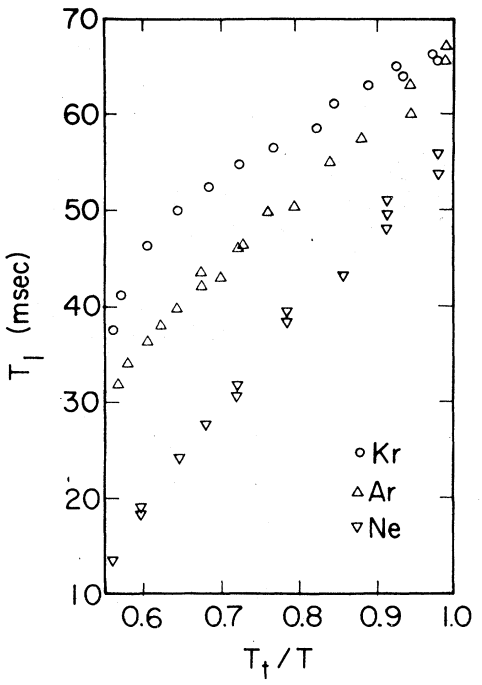


FIG. 8. $T_1$ of $o$-$H_2$ in liquid, neon, argon, and krypton.

## IV. RELAXATION TIMES

The measured values of $T_1$ and $T_2$ were found to be equal in each case to within ±3%, and apparently reflect extreme narrowing. The data do not show any appreciable concentration dependence, indicating that the proton relaxation times obtained here for samples between 0.03% and 0.8% correspond essentially to zero concentration of $H_2$. Figure 8 shows the observed spin-lattice relaxation times $T_1$ as functions of $1/T^*$ in liquid neon, argon, and krypton.

The proton-spin relaxation of $o$-$H_2$ in the liquids studied here arises from the intramolecular spin interactions, modulated by rotational motion of the $H_2$ molecules. The intermolecular contribution to the relaxation rate $1/T_1$ is of the order of (3000 sec)$^{-1}$, and clearly is negligible. There are two intramolecular spin interactions of roughly equal strengths: The proton-proton magnetic dipole interaction and the spin-rotation interaction which involves the net nuclear spin and the rotation of the molecule. The temperatures used in the present experiments were below 210 K, and the rotational motion of $o$-$H_2$ to good approximation is restricted to the $J=1$ manifold, because the first excited rotational level with $J=3$ is 860 K higher. At 200 K, 3% of the $o$-$H_2$ are in the $J=3$ states. In effect, the physical system is equivalent to a nuclear spin $I=1$ coupled to a molecular (rotational) spin $J=1$. The molecular spin $J$ is relaxed by interaction with host atoms. Intermolecular collisions induce transitions between the three $m_J$ sublevels of the $J=1$ rotational manifold. Since these transitions are caused only by the relatively weak anisotropic part of the $H_2$–rare-gas intermolecular potential, $T_1$ measurements serve to probe this part of the intermolecular interaction, which usually is too weak to have any appreciable effect on diffusion and other transport properties. This relaxation mechanism has been studied extensively in pure gaseous and liquid hydrogen as well as other systems.[36-38]

Hardy[37] showed that the motion of the molecular spin ($J=1$) can be described by two correlation times $\tau_1$ and $\tau_2$. These are the time constants of the exponentially decaying correlation functions of first-order and second-order multipole $J$ operators, respectively. $\tau_1$ and $\tau_2$ are related by a constant multiplicative factor. Measurements of the density dependence of $T_1$ and $T_2$ for the low-density normal $H_2$ gas indicate that $0.6 \leq \tau_1/\tau_2 < 1.0$.[37,39,40] Bloom and Oppenheim[38] obtained a theoretical value of $\tau_1/\tau_2 = 0.6$ for systems restricted to $J=1$. These correlation times also are related to the transition rates $W_1$ for $\Delta m_J = \pm 1$ and $W_2$ for $\Delta m_J = \pm 2$ in the $J=1$ manifold: $1/\tau_1 = W_1 + 2W_2$ and $1/\tau_2 = 3W_1$.[37,38] Computer cross-section calculations of $H_2$–rare-gas atom collisions give $W_2 = 2W_1$ and again yield $\tau_1/\tau_2 = 0.6$ for hydrogen with $J=1$.[42]

Hardy derived expressions for $T_1$ and $T_2$ in terms of $\tau_1$ and $\tau_2$.[37] For $\tau_1/\tau_2 = 0.6$, in the limit of $\tau_1$ much smaller than the Larmor period (extreme narrowing), $T_1 = T_2$ and

$$1/T_1 = 3.9 \times 10^{12} \tau_1 , \quad (4)$$

where $T_1$ and $\tau_1$ are measured in seconds.

Equation (4) can be used to derive values of $\tau_1$ from the $T_1$ data of Fig. 8. The resulting molecular correlation times $\tau_1$ fall in the range between 4 and 20 psec, and are shown in Fig. 9. As expected for the nearly spherical $H_2$, these times are considerably longer than the mean times between collisions in dense gases or the kinetic correlation times of liquids in the same temperature range.

For $H_2$ in the extreme narrowing regime, $T_1$ should be inversely proportional to the mean time between collisions $\bar{\tau} \propto 1/\rho$. At constant temperature, therefore, $T_1/\rho$ should remain independent of density as long as the density is large enough to give extreme narrowing conditions, but not sufficiently large for three-particle collisions to become important. For $H_2$ this density range typically extends from a few amagats[37] to as high as several hundred amagats.[41] The temperature dependence of $T_1/\rho$, in real gas hosts, should also reflect any velocity dependence of $J$-reorienting collision cross sections.[42] In very dense gases and in liquids the behavior of $T_1/\rho$ is expected to be rather complicated, because multiple-particle interactions play an important role in inducing transitions between $m_J$ sublevels. Where the data are available, the variations in $T_1/\rho$ with temperature and density should be analyzed separately. In the present experiments, however, these variations cannot be separated because measurements have been made at saturated vapor pressure of the host liquid with a small overpressure of hydrogen. In the analysis of these data it is useful, nevertheless, to compare $T_1/\rho$ values at the same temperature for $H_2$ in different gas and liquid hosts.

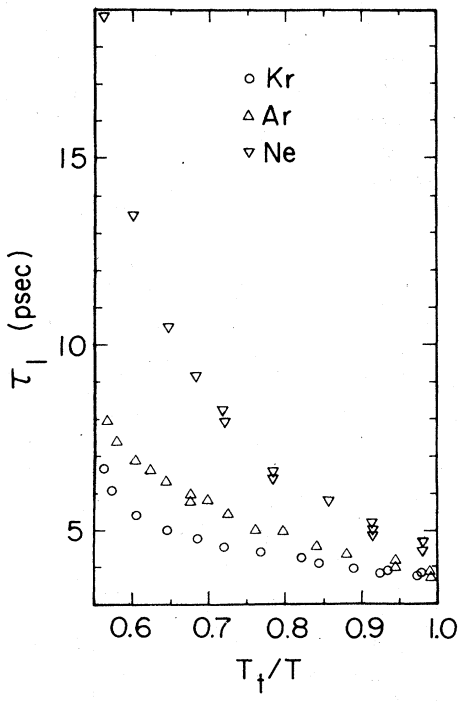


FIG. 9. $\tau_1$ of $o$-$H_2$ in liquid neon, argon, and krypton derived from Eq. (4).

Measurements of $T_1/\rho$ for various gas-phase dilute $H_2$–rare-gas mixtures have been reported in the literature.[4,5,43-45] Riehl *et al.*[43] measured $T_1/\rho$ for $H_2$-He mixtures in the range 77–300 K. Lalita and Bloom[44] extended $H_2$-He measurements to 730 K, and Bloom[45] reported an $H_2$-He measurement at 20.4 K. Foster and Rugheimer[4] determined $T_1/\rho$ for $H_2$ in neon, argon, krypton, and xenon between 165 and 265 K using gas densities of about 20 amagats. The earlier $H_2$-Ne and $H_2$-He gas-mixture results of Williams[5] have substantial scatter, and disagree somewhat with the subsequent results.[4,43] Measurements of $T_1$ for various concentrations of $o$-$H_2$–$p$-$H_2$ gas mixtures were made by Lipsicas and Hartland[6] at temperatures between 20 and 400 K.

Values of $T_1/\rho$ derived from the present $T_1$ measurements for dilute $H_2$ in liquid neon, argon, and krypton are plotted as open symbols in Fig. 10. The various lines drawn in the figure indicate for comparison some reported results for gas-phase $H_2$ and $H_2$–rare-gas mixtures. The dashed lines indicate the $T_1/\rho$ results of Foster and Rugheimer[4] for $H_2$ extrapolated to zero concentration in gas-phase neon, argon, krypton, and xenon. Also shown by a dashed line are the $H_2$-He gas results of Riehl *et al.*[43] The dot-dashed line shows theoretical results quoted by Lalita and Bloom[44] for dilute $H_2$-He gas mixtures. The cross indicates Bloom's earlier $H_2$-He gas measurement[45] at 20.4 K. The solid line shows the Lipsicas and Hartland[6] $T_1/\rho$ results extrapolated to infinitely dilute $o$-$H_2$–$p$-$H_2$ gas mixtures. At the lower left-hand side, solid dots indicate $T_1/\rho$ reported[7] for dilute $o$-$H_2$ in liquid $p$-$H_2$ at SVP.

Direct comparison between liquid and gas values of $T_1/\rho$ at the same temperature can be made in the case of $H_2$-Kr. Foster and Rugheimer's measurements[4] for Kr gas (20 amagats) near the critical temperature (209.5 K) give $(T_1/\rho)_{gas} \simeq 110$ μsec/amagat, in approximate agreement with the present liquid data indicated by open circles in Fig. 10. Apparently, $(T_1/\rho)_{gas}$ for $H_2$-Kr has little

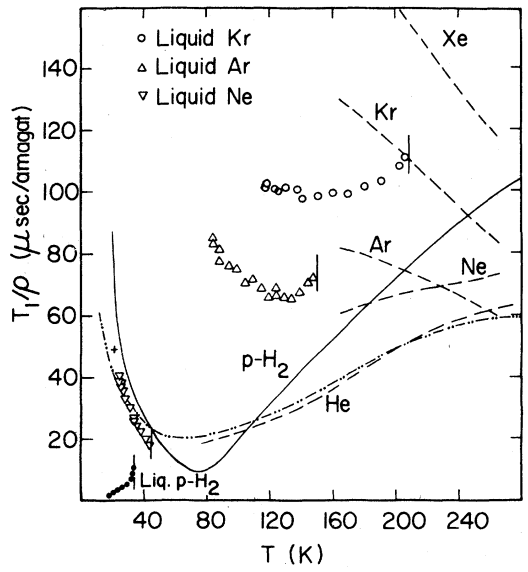


FIG. 10. $T_1/\rho$ for $o$-$H_2$ in neon, argon, krypton, and $p$-$H_2$. The dashed lines are for $H_2$ extrapolated to zero concentration in gaseous $H_2$–rare-gas mixtures (Refs. 4 and 43). The cross indicates a $H_2$-He gas result (Ref. 45). The dot-dashed line shows theoretical results quoted for $H_2$-He gas mixtures (Ref. 44), and the solid line indicates experimental results for $T_1$ in infinitely dilute $o$-$H_2$–$p$-$H_2$ gas mixtures (Ref. 6). The solid dots indicate results for dilute $o$-$H_2$–$p$-$H_2$ liquid mixtures (Ref. 7).

variation with density between 20 amagats and the critical density, 245 amagats. The decrease of $(T_1/\rho)_{\text{liquid}}$ below $(T_1/\rho)_{\text{gas}}$ at lower temperatures reflects the importance of many-body collisions in the dense liquid.

The $(T_1/\rho)_{\text{gas}}$ data for $H_2$ in argon gas do not extend into the liquid-argon temperature range (Fig. 10). However, a short extrapolation of the slowly varying $(T_1/\rho)_{\text{gas}}$ results indicates a probable value of 82 μsec/amagat near $T_c$ (150.7 K). The trend of the present $H_2$-Ar $(T_1/\rho)_{\text{liquid}}$ data in this region also can be extrapolated to a value consistent with the gas result. As is the case for $H_2$ in liquid krypton, $(T_1/\rho)_{\text{liquid}}$ for $H_2$ in liquid argon becomes smaller than $(T_1/\rho)_{\text{gas}}$ as the temperature decreases and the liquid density increases. It appears that the many-body effects in the liquids decrease $T_1/\rho$ by no more than 30%.

There are no reported $T_1$ data for gaseous $H_2$-Ne mixtures in the liquid-neon temperature range. Williams[5] reported $(T_1/\rho)_{\text{gas}} \simeq 35$ μsec/amagat near 50 K. However, his results at higher temperatures are about twice as large as the $H_2$-Ne gas results of Foster and Rugheimer[4] indicated in Fig. 10. It would be particularly interesting to have $(T_1/\rho)_{\text{gas}}$ for $o$-$H_2$–Ne in the range of liquid-neon temperatures because the intermolecular potential parameters of Ne and $H_2$ are similar.[32,33] Ne atoms should play a role similar to that of molecules of $p$-$H_2$ in the anisotropic interaction with $o$-$H_2$ molecules at temperatures where $p$-$H_2$ molecules are in the $J=0$ state. On this basis, values of $T_1/\rho$ should be approximately equal for dilute $o$-$H_2$ in $p$-$H_2$ gas and in neon gas. Indeed, near 182 K the experimental values are 64 μsec/amagat in both systems (Fig. 10). As the temperature is decreased, however, $T_1/\rho$ for $p$-$H_2$ appears to decrease more rapidly than for neon (although this is not true for the earlier $H_2$-Ne data of Williams[5]).

$T_1/\rho$ values[7] for dilute $o$-$H_2$ in liquid $p$-$H_2$ (Fig. 10) are much smaller than for dilute $o$-$H_2$ in gaseous $p$-$H_2$ at the same temperature, and the two sets of data have different temperature dependences. It has been proposed[7,46,47] that the $p$-$H_2$ host molecules surrounding an isolated $o$-$H_2$ in the liquid present a spherically symmetric potential for the $o$-$H_2$. The symmetry reduces the transition rate among the three $J=1$ sublevels of the $o$-$H_2$ and decreases the observed $T_1$. This explanation should apply equally well to the $H_2$–rare-gas systems studied here. However, in $H_2$-Ar and $H_2$-Kr mixtures, $T_1/\rho$ is approximately the same in the gas and liquid phases. Because Ne and $p$-$H_2$ are so similar, it would be very interesting to compare $T_1/\rho$ for gas and liquid $H_2$-Ne systems. If we assume that $T_1/\rho$ of $H_2$ in Ne gas roughly equals that of $o$-$H_2$ in $p$-$H_2$ gas (Fig. 10), then $T_1/\rho$ of dilute $H_2$ in Ne is approximately equal in the gas and liquid phases. The source of this qualitative distinction between liquid $p$-$H_2$ and liquid Ne (and the other rare-gas liquids) as hosts for $o$-$H_2$ might be quantum mechanical ($H_2$ is light) or the nonspherical nature of the $p$-$H_2$ molecules. Clearly any conclusions require $T_1/\rho$ data for dilute $H_2$ in Ne gas in the liquid-temperature range.

Riehl *et al.*[43] have pointed out in their study of proton relaxation in gaseous $H_2$-He mixtures that in general a $T_1/\rho$ minimum in gas mixtures is to be anticipated on the basis of reasonable intermolecular potentials. The $T_1/\rho$ minimum is expected to occur at temperatures where the Maxwellian distribution has a maximum near relative molecular velocities for which the reorientation cross section for $\Delta m_J = \pm 1$ transitions within the $J=1$ manifold of $o$-$H_2$ has a sharp minimum.[42] The results of the present experiments shown in Fig. 10 indicate that for $H_2$-Ar and $H_2$-Kr liquid mixtures, minima in $T_1/\rho$ occur near $kT/\epsilon = 1.8$ (Table III). Here $\epsilon$ has been taken to be the isotropic potential parameter determined by Helbing *et al.*[48] for $H_2$–rare-gas scattering. The approximate temperatures corresponding to the $T_1/\rho$ minima in liquid

TABLE III. Isotropic potential parameters and temperature of $T_1/\rho$ minima for liquid-phase dilute $H_2$-rare-gas mixtures.

| | $a$ (Å) | $\epsilon/k$ (K) | $T_{min}$ (K) | $kT_{min}/\epsilon$ |
|---|---|---|---|---|
| He | 2.75[a] | 20.0[a] | | |
| Ne | 2.73[b] | 30.8[b] | | |
| Ar | 2.98[b] | 73.2[b] | 131 | 1.79 |
| Kr | 3.25[b] | 78.9[b] | 145 | 1.84 |
| Xe | 3.47[b] | 86.2[b] | | |

[a] I. Amdur and A. P. Malinauskas, J. Chem. Phys. 42, 3355 (1965).
[b] Reference 48.

argon and krypton have been determined by drawing smooth curves through the data of Fig. 10. A hypothetical $T_1/\rho$ minimum near $kT/\epsilon = 1.8$ also is consistent with the present $H_2$-Ne liquid-mixture data ($1.8\epsilon/k = 55$ K for Ne).

The Bloom-Oppenheim theory[38] of nuclear-spin relaxation arising from the anisotropic interaction between a host gas and $o$-$H_2$ molecules yields the expression[5,6]

$$T_1 \propto a^4\rho\left(\frac{\mu}{T}\right)^{1/2} E^2 \int_0^\infty F(y)dy\,. \tag{5}$$

Here $\mu$ is the reduced mass, $E$ is the strength of the anisotropic interaction at $r = a$ (the Lennard-Jones parameter), and the integral is over the radial distribution function and the anisotropic interaction.

According to Eq. (5) the quantity $\xi = T_1 T^{1/2}/\rho a^4 \mu^{1/2}$ should reflect many-body effects and the temperature and host dependence of $E^2\int_0^\infty F(y)dy$. At temperatures below 200 K more than 96% of the $o$-$H_2$ molecules are in the $J = 1$ states, and $\xi$ is the same (except for a multiplying constant) as the parameter $k_0$ discussed by Bloom *et al.*[49]

Bloom-Oppenheim theory has been shown to be useful in correlating $T_1$ data for $H_2$ in gas-phase rare gases,[4] and it is of some interest to examine the same correlation in the more complicated case of liquid mixtures. Figure 11 shows some of the liquid and gas data of Fig. 10 replotted as $\xi = T_1 T^{1/2}/\rho a^4 \mu^{1/2}$. The abscissa has been inverted and reduced to $\beta\epsilon = \epsilon/kT$. Here $a$ and $\epsilon$ are the isotropic $H_2$-rare-gas potential parameters from Table III. The present results for $H_2$-rare-gas liquids again are indicated by open symbols. The solid lines indicate the gas-phase $H_2$-rare-gas results in neon, argon, krypton, and xenon (Foster and Rugheimer[4]) and in helium (Riehl *et al.*[43]). The cross again indicates Bloom's result[45] for $H_2$-He at 20.4 K. The dashed curve indicates the theoretical $H_2$-He curve sketched by Lalita and Bloom.[44]

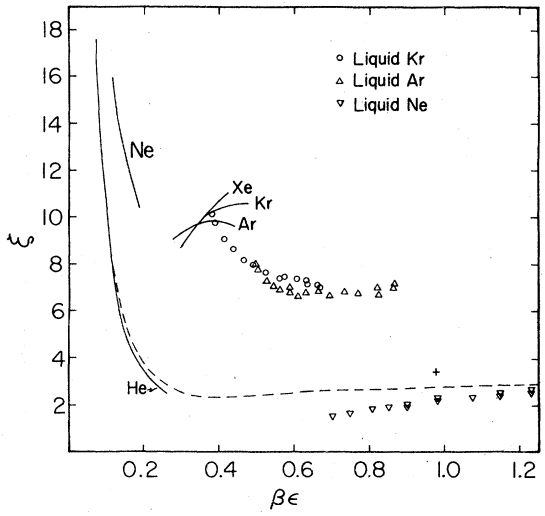


FIG. 11. Quantity

$$\xi = T_1\sqrt{T}/a^4\rho\sqrt{\mu}\,[\mu\text{sec (mole K/g)}^{1/2}\,\text{Å}^{-4}\,\text{amagat}^{-1}]$$

for $o$-$H_2$ in helium, neon, argon, and krypton as a function of reduced reciprocal temperature. Results for liquid mixtures are indicated by open symbols. Gas values for $H_2$-rare-gases are indicated by solid lines (Refs. 4 and 43). The dashed line is a theoretical $H_2$-He gas result (Ref. 44) and the cross a $H_2$-He-gas experimental result (Ref. 45).

Clearly the extension of dilute-gas Bloom-Oppenheim theory to the present $H_2$–rare-gas liquid results has some success. The present data for liquid argon and krypton essentially coincide in Fig. 11, and their temperature variation at low temperatures seems consistent with that of the liquid-neon data, which fall on the low-temperature side of the $T_1/\rho$ minimum in Fig. 10. The liquid densities for the data points shown range from 339 amagats for liquid Kr near $T_c$ to 1380 amagats for liquid Ne near $T_t$. Many-body collisions must play a role, and the gas model on which Eq. (5) is based probably is inadequate. Nevertheless, the Bloom-Oppenheim gaslike model in the constant-acceleration approximation previously has been found useful in discussing liquid relaxation results (e.g., Miller *et al.*[7] and Lipsicas and Hartland[6] in discussing liquid $o$-$H_2$–$p$-$H_2$ mixtures). Figure 11 also emphasizes the correspondence between the $H_2$-Ne and $H_2$-He results for both gas and liquid mixtures.

The increase in $\xi$ at high temperatures (small $\beta\epsilon$) has been discussed by Lalita *et al.*[50] Presumably $\xi$ for $H_2$-Ar, -Kr, and -Xe gas mixtures turns rapidly upwards below $\beta\epsilon = 0.25$ in Fig. 11. In the present experiments on liquid mixtures, $\xi$

depends (in the constant-acceleration approximation) on the radial distribution function and on $V_2(r)$, the coefficient of the anisotropic term in the potential energy of interaction between a $H_2$ molecule and a rare-gas atom.[44] Foster and Rugheimer[4] have interpreted their gas-mixture relaxation results to indicate that Bloom-Oppenheim theory implies slightly different radial dependences for the anisotropic potentials in the various $H_2$–rare-gas mixtures.

## V. SUMMARY

The diffusion of dilute $H_2$ in liquid neon, argon, and krypton is more rapid than the self-diffusion of each host liquid. Near the triple points the $H_2$ diffusion has the same activated temperature dependence as the host diffusion. The ratios of the $H_2$ diffusion to the host self-diffusion increase as the critical points are approached, the ratios becoming nearly the same for the three liquid mixtures. The diffusion ratio observed for $H_2$-Kr is in satisfactory agreement with the results of hard-sphere molecular dynamics.[31] For $H_2$-Ne and $H_2$-Ar the observed temperature variation of the diffusion ratio appears to be significantly larger than the molecular-dynamics result. Measurements of self-diffusion in liquid neon near the critical point are needed in order to strengthen this conclusion.

Proton spin relaxation in the dilute liquid mixtures shows systematic variations with temperature and density that can be correlated with Bloom-Oppenheim gaslike relaxation theory[38,50] and with relaxation results for gaseous $H_2$–rare-gas mixtures and $o$-$H_2$–$p$-$H_2$ mixtures. Evidently, three-body and higher-order collisions do not play a large role in the rotational relaxation of $H_2$ in rare-gas liquids. This is quite unlike the situation in dilute liquid solutions of $o$-$H_2$ in $p$-$H_2$.[7,47] The difference may arise from quantum effects in the $o$-$H_2$–$p$-$H_2$ case or from the nonspherical nature of the individual $p$-$H_2$ molecules.

## ACKNOWLEDGMENTS

The authors have benefited from conversations with B. J. Alder, M. Bloom, P. A. Fedders, and H. Meyer. This work was supported in part by the NSF and a Navy Equipment Loan Contract. One of us (M.S.C.) was supported by a NSF Graduate Fellowship.

---

*Present address: Chemistry Division, Oak Ridge National Laboratory, Oak Ridge, Tenn.

[1]G. Cini-Castagnoli and F. P. Ricci, Nuovo Cimento 15, 795 (1960).
[2]F. P. Ricci, Phys. Rev. 156, 184 (1967).
[3]G. Cini-Castagnoli, A. Giardini-Guidoni, and F. P. Ricci, Phys. Rev. 123, 404 (1961).
[4]K. R. Foster and J. H. Rugheimer, J. Chem. Phys. 56, 2632 (1972).
[5]D. L. Williams, Can. J. Phys. 40, 1027 (1962).
[6]M. Lipsicas and A. Hartland, Phys. Rev. 131, 1187 (1963).
[7]C. E. Miller, T. M. Flynn, T. K. Grady, and J. S. Waugh, Physica 32, 244 (1966).
[8]M. S. Conradi, K. Luszczynski, and R. E. Norberg (unpublished).
[9]W. B. Streett and C. H. Jones, J. Chem. Phys. 42, 3989 (1965).
[10]J. C. Mullins and W. T. Zeigler, in *Advances in Cryogenic Engineering*, edited by K. D. Timmerhaus (Plenum, New York, 1965), Vol. 10, p. 171.
[11]C. J. Sterner, Rev. Sci. Instrum. 31, 1159 (1960).
[12]T. O. Niinikoski, Rev. Sci. Instrum. 43, 430 (1972).
[13]H. Volk and G. D. Halsey, Jr., J. Chem. Phys. 33, 1132 (1960).
[14]W. G. Clark, Rev. Sci. Instrum. 35, 316 (1964).
[15]M. S. Conradi, J. Magn. Reson. 23, 165 (1976).
[16]E. O. Stejskal, Rev. Sci. Instrum. 34, 971 (1963).
[17]J. E. Opfer, Ph.D. thesis (Washington University, 1966) (unpublished).
[18]J. S. Murday, J. Magn. Reson. 10, 111 (1973).
[19]R. K. Crawford, in *Rare Gas Solids*, edited by M. L. Klein and J. A. Venables (Academic, London, 1977), Vol. 2, p. 663.
[20]R. Henry and R. E. Norberg, Phys. Rev. B 6, 1645 (1972).
[21]L. Bewilogua, C. Gladun, and B. Kubsch, J. Low Temp. Phys. 4, 299 (1971).
[22]J. Naghizadeh and S. A. Rice, J. Chem. Phys. 36, 2710 (1962).
[23]D. F. Cowgill and R. E. Norberg, Phys. Rev. B 13, 2773 (1976).
[24]O. J. Eder, S. H. Chen, and P. A. Egelstaff, Proc. Phys. Soc. 89, 833 (1966).
[25]R. S. Ehrlich, Ph.D. thesis (Rutgers University, 1969) (unpublished).
[26]R. S. Ehrlich and H. Y. Carr, Phys. Rev. Lett. 25, 341 (1970).
[27]J. D. Noble and M. Bloom, Phys. Rev. Lett. 14, 250 (1965).
[28]A. C. Hollis Hallett, in *Argon, Helium, and the Rare Gases*, edited by G. A. Cook (Interscience, New York, 1961), Vol. 1, p. 313; and A. C. Jenkins, *ibid.*, p. 391.
[29]E. Helfand and S. A. Rice, J. Chem. Phys. 32, 1642 (1960).
[30]J. A. Barker, in *Rare Gas Solids*, edited by M. L. Klein and J. A. Venables (Academic, London, 1976), Vol. 1, p. 260.
[31]B. J. Alder, W. E. Alley, and J. H. Dymond, J. Chem. Phys. 61, 1415 (1974).
[32]J. D. Rogers and F. G. Brickwedde, J. Chem. Phys. 42, 2822 (1965).
[33]J. D. Rogers and F. G. Brickwedde, Physica 32, 1001 (1966).

[34]L. L. Lee and D. Levesque, Mol. Phys. 26, 1351 (1973).
[35]D. Levesque and L. Verlet, Phys. Rev. A 2, 2514 (1970).
[36]A. Abragam, *Principles of Nuclear Magnetism* (Oxford University, London, 1961).
[37]W. N. Hardy, Can. J. Phys. 41, 1580 (1963).
[38]M. Bloom and I. Oppenheim, Can. J. Phys. 41, 1580 (1963).
[39]K. E. Kisman and R. L. Armstrong, Can. J. Phys. 52, 1555 (1974).
[40]R. L. Armstrong, K. E. Kisman, and W. Kalechstein, Can. J. Phys. 53, 1 (1974).
[41]M. Lipsicas and M. Bloom, Can. J. Phys. 39, 881 (1961).
[42]J. K. Kinsey, J. W. Riehl, and J. S. Waugh, J. Chem. Phys. 49, 5269 (1968).
[43]J. W. Riehl, J. L. Kinsey, J. S. Waugh, and J. H. Rugheimer, J. Chem. Phys. 49, 5276 (1968).
[44]K. Lalita and M. Bloom, Can. J. Phys. 49, 1018 (1971).
[45]M. Bloom, Physica 23, 237 (1957).
[46]J. M. Deutch and I. Oppenheim, J. Chem. Phys. 44, 2843 (1966).
[47]M. Lipsicas and A. Hartland, J. Chem. Phys. 44, 2839 (1966).
[48]R. Helbing, W. Gaide, and H. Pauly, Z. Phys. 208, 215 (1968).
[49]M. Bloom, I. Oppenheim, M. Lipsicas, G. Wade, and C. Yarnell, J. Chem. Phys. 43, 1036 (1965).
[50]K. Lalita, M. Bloom, and J. Nobel, Can. J. Phys. 47, 1335 (1969).